

## **SEISMIC PERFORMANCE OF SHAPE MEMORY ALLOY REINFORCED CONCRETE DUAL SYSTEMS**

Emad A. ABRAIK<sup>1</sup>, Maged A. YOUSSEF<sup>2</sup>

### **ABSTRACT**

A reinforced concrete (RC) dual system utilizes RC walls in conjunction with RC frames to resist seismic loads. High energy dissipation and low seismic deformations are its characteristics. This paper evaluates the effect of utilizing superelastic shape memory alloy (SE-SMA) bars on the engineering demand parameters of RC dual systems. Two steel RC dual systems are designed. The designs are then revised using SE-SMA bars. Two potential layouts for the locations of SE-SMA bars are examined, which resulted in four SE-SMA dual systems. Incremental dynamic analysis (IDA) is then conducted. SE-SMA RC dual systems are found to have superior seismic performance as compared to steel RC systems.

*Keywords: Dual system; Shape memory alloy; Incremental dynamic analysis*

### **1. INTRODUCTION**

Dual systems combining reinforced concrete (RC) frames and RC walls are widely adopted in tall buildings. During seismic excitations, frames deform in a shear mode, restraining deformations of the upper stories, whereas walls deform in a bending mode with the upper stories experiencing the highest drifts. Therefore, the combined deformation shape is expected to follow a flexural profile in the lower stories and shear profile in the upper stories. The seismic response of frame-wall dual systems is sensitive to their relative stiffness. The 1985 edition of the NBCC used the term dual system, when the base shear resisted by the frames is not less than 25% of the total base shear.

Several research studies investigated the seismic design of RC dual systems (Emori and Schnobrich 1978; Goodsir et al. 1982; Aktan and Bertero 1984; Tuna et al. 2012). The life-safety seismic performance target leaves these systems vulnerable to severe damage characterized by large permanent residual displacements.

Tremendous efforts have been devoted to mitigate the seismic damage and reduce the repair cost of seismically-damaged RC structures by utilizing SE-SMA material (Youssef et al. 2008; Saiidi et al. 2008; Alam et al. 2008; Tazarv and Saiidi 2013). Abdulridha (2012) confirmed experimentally that SE-SMA bars significantly reduce the seismic residual deformations for RC walls. Abraik and Youssef (2015) identified the performance of SE-SMA RC squat and intermediate walls considering different SE-SMA bar locations. Abraik and Youssef (2016) assessed the performance of three-story SE-SMA cantilever wall, located in a high seismic zone. Results indicated that location of SE-SMA bars has a significant effect on the mitigation of residual displacements.

This study is the first to evaluate the seismic response of dual systems that utilize SE-SMA bars. Both local and global responses are evaluated using: wall strains, beam and column strains, axial loads, shear forces, bending moments, inter-story drifts, and residual drifts.

---

<sup>1</sup>Graduate Student Researcher, Western University, London, Canada, [eabraik@uwo.ca](mailto:eabraik@uwo.ca)

<sup>2</sup>Professor, Civil and Environmental Department, Western University, London, Canada, [youssef@uwo.ca](mailto:youssef@uwo.ca)

## 2. NUMERICAL MODEL AND FAILURE CRITERIA

A 2D nonlinear model is used for steel RC walls and steel moment frames using Open System for Earthquake Engineering Simulation software (OpenSees, 2004). The walls are modeled using the Shear-Flexural Interaction Multi Vertical Line Element Model (SFI-MVLEM) that is shown in Figure 1. The element is based on the concept of MVLEM, which captures the axial-flexural interaction through the axial deformations of each element and the relative rotations between the top and the bottom faces of each element (Kolozvari, 2013). The model assumes that the relative rotation happens at 40% of the element height. The SFI-MVLEM captures the shear flexural interaction by transferring the shear deformations to that point. The RC frames are modeled using the nonlinear force-based fiber frame element that has five integration points. The RC walls and the RC frames are then connected by a rigid link at each story.

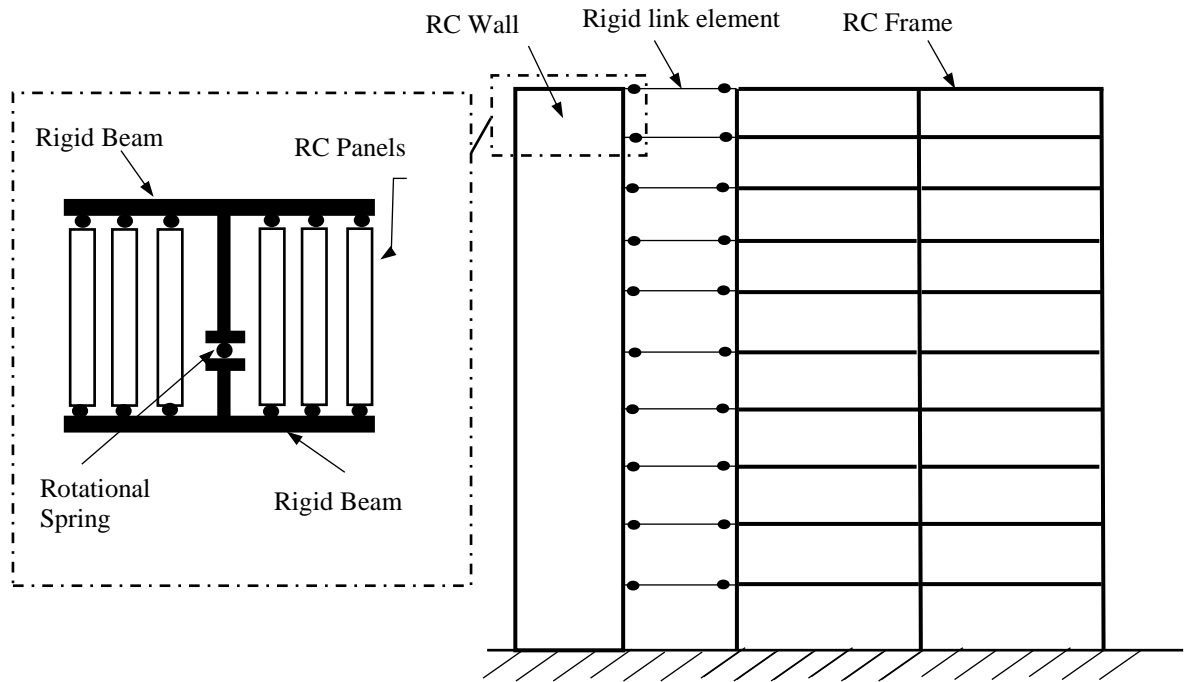


Figure 1. Dual system numerical model

The global failure criteria specified by PEER-TBI (2017) are adopted in this research. The mean and the maximum inter-story drifts are limited to 3.0% and 4.5%, respectively. The mean and maximum residual drifts ratio should not exceed 1.0% and 1.5%, respectively. Strains are utilized to identify local failures. The tensile steel strain at fracture of steel is 5.0%, while the maximum compressive concrete strain is 2% (Panagiotou 2008).

The modulus of elasticity of SE-SMA bars ( $E_{SMA}$ ), the stress at which inelastic deformations initiate ( $f_{SMA}$ ), and the post-yield strength are assumed to be 38,000 MPa, 380 MPa, and 1725 MPa, respectively. SE-SMAs have the ability to recover their original shape after being deformed to an ultimate strain of 6 to 8% (Hurlebaus and Gaul, 2006). A strain of 7% is used to define their ultimate strain.

### 2.1 Numerical Model Validation

An experimental shake table test of a slender eight-story RC wall (Ghorbanirenani et al. 2012) is selected to validate the analytical model. The selected wall is designed according to NBCC (2005) with a force reduction factor of 2.8. A simulated time history ground motion, developed for eastern North America, has been used to test the wall. Eight SFI-MVL elements are used to model the tested wall. The predicted

analytical results agree well with the experimental results as shown in Figure 2.

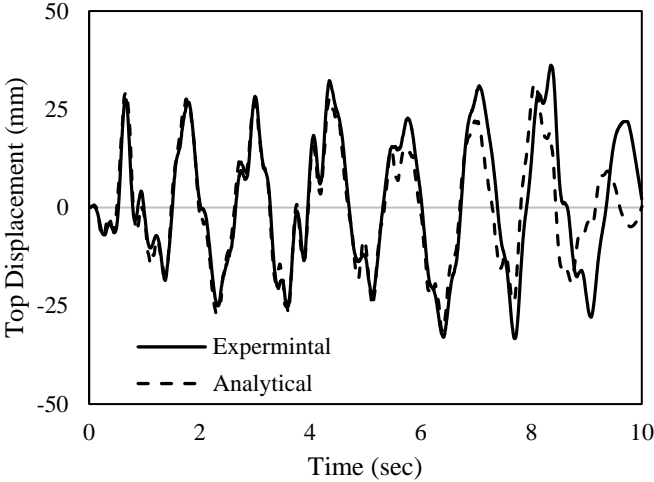


Figure 2. Top displacement of RC wall tested by Ghorbanirehani (2012)

**2.2 Dual-System Design**

The plan view of the assumed 10-story building is shown in Figure 3. The lateral resisting system utilizes two RC walls and two ductile RC frames in each direction. The story height is 3.0 m. The considered building is assumed to be located in Vancouver, BC, with soil class D. The peak ground acceleration (PGA) is equal to 0.46g. Concrete compression strength is 30 MPa and steel yield strength is 400 MPa. The structural lumped mass at each story includes self-weight and 25% of the applied live load.

Two steel RC dual-systems are designed according to the requirement of NBCC (2015) and A23.3 (2014). The difference between the two buildings (BL1 and BL2) is the percentage of seismic loads resisted by the RC walls (75% for BL1 and 50% for BL2).

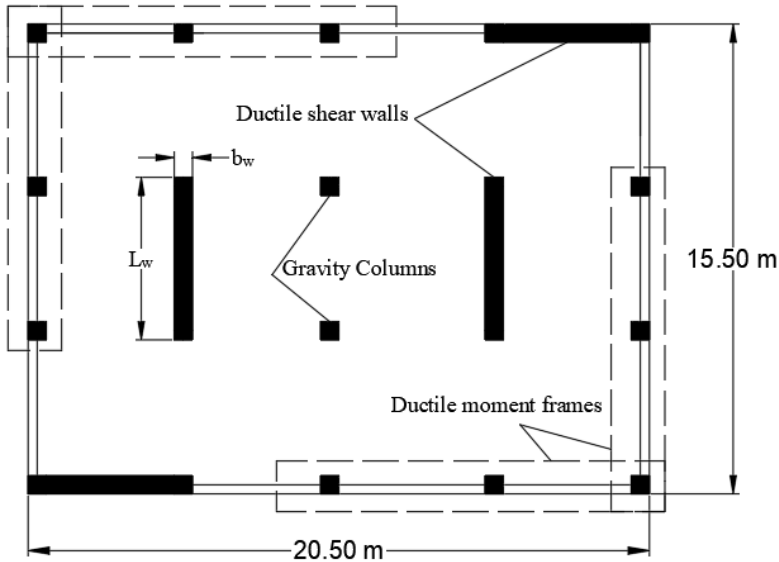


Figure 3. Typical floor plan (dimensions in m)

The cross-section of the beams is 400 mm by 600 mm. The ratio of the longitudinal top and bottom steel bars is 0.55%. BL1 has column dimensions of 700 mm by 700 mm for the first five floors and 600 mm by 600 mm for the remaining floors. BL2 has column size of 800 mm by 800 mm for floors 1 to 5 and

700 mm by 700 mm for floors 6 to 10. The design details of the RC walls are presented in Table 1.

Table 1. RC walls design details.

Building	Period	$L_w$ (mm)	$b_w$ (mm)	$\rho_h$ (%)	$\rho_{hb}$ (%)	$\rho_v$ (%)	$\rho_{vb}$ (%)
BL1	1.15	2800	300	0.33	0.55	0.33	1.0
BL2	1.29	1800	300	0.66	0.66	0.33	1.0

where  $L_w$ ,  $b_w$ ,  $\rho_h$ ,  $\rho_{hb}$ ,  $\rho_v$ , and  $\rho_{vb}$  are the wall length, wall thickness, horizontal steel ratio in the web, horizontal steel ratio in the boundary elements, vertical steel ratio in the web, and vertical steel ratio in the boundary elements.

The investigated locations for SE-SMA bars, illustrated in Figure 4, are: (1) SE-SMA bars at the wall critical sections [BL1SW and BL2SW] and (2) SE-SMA bars at the wall critical sections and at the ends of the 1st and 7th story beams [BL1SWF and BL2SWF]. Mechanical couplers are assumed to connect SE-SMA bars with conventional steel reinforcement.

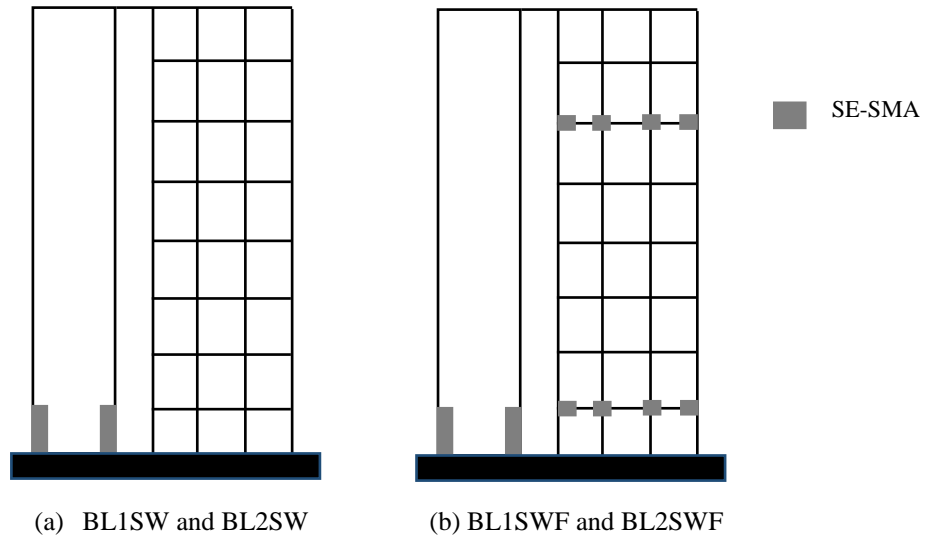


Figure 4. Locations of SE-SMA bars

### 3. GROUND MOTIONS SELECTION

Figure 5 presents the mean spectra acceleration of seven sets of ground motions, scaled to the design spectrum of Vancouver, British Columbia, assuming 5% damping ratio. Mean square error (MSE) is used to scale the chosen ground motions. Soil class D and shear wave velocity of 360 m/s are assumed. The ground motions are selected to represent a range between  $0.2T_{1s}$  and  $1.5T_1$ , where  $T_{1s}$  and  $T_1$  are the minimum and maximum fundamental periods of the BL1 and BL2, respectively. Incremental dynamic analysis (IDA) is then carried out using the seven sets of the selected ground motions. Each dual system is subjected to increasing amplitudes of each of the horizontal components of the considered earthquakes until failure. The Intensity Measure (IM), which represents the spectral acceleration  $S_{a(\text{design})}$  at the first period, ranges from  $0.38g [S_{a(\text{design})}]$  to  $1.15g [S_{a(\text{max})}]$  for BL1 and from  $0.16g [S_{a(\text{design})}]$  to  $0.60g [S_{a(\text{max})}]$  BL2.

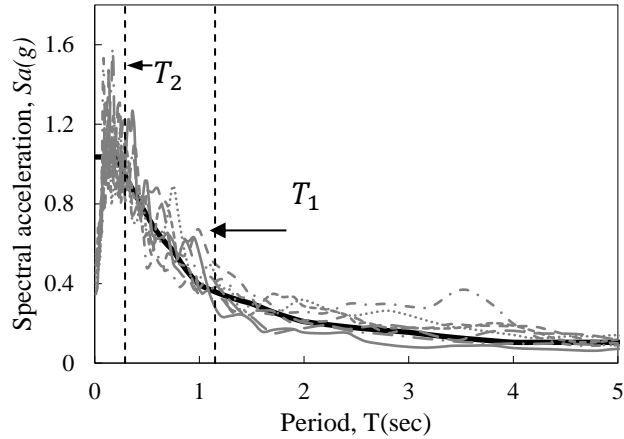


Figure 5. Spectra acceleration of scaled ground motions

## 4. NONLINEAR TIME HISTORY ANALYSIS RESULTS

### 4.1 Wall Local Response

Figure 6 plots the strain profile for BL1 and BL2 subjected to two intensity hazard levels [ $S_{a(\text{design})}$  and  $S_{a(\text{max})}$ ]. The wall tensile strain profile shows an elastic response for low-intensity ground motions [ $S_{a(\text{design})}$ ]. Increasing the intensity level to  $S_{a(\text{max})}$  leads to the formation of a plastic hinge at the base with a length of about 10% of the wall height.

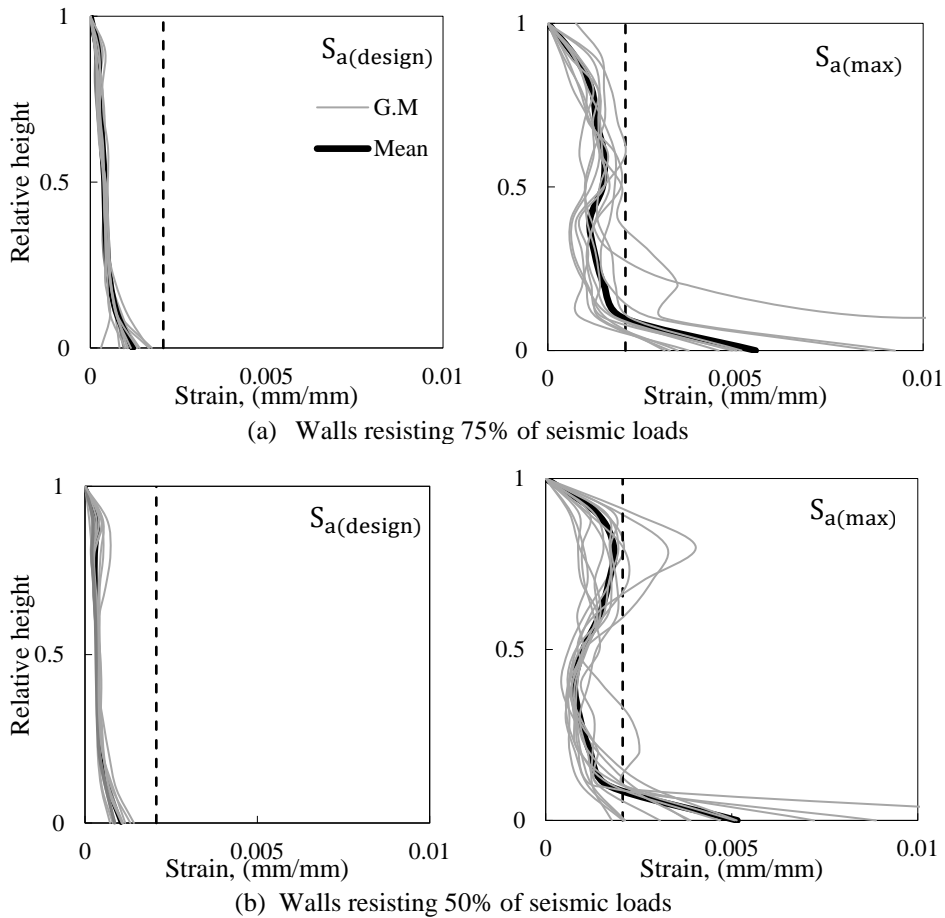


Figure 6. Mean reinforcement tensile strain in the 10-story steel RC wall

Figure 7 plots the bending moments and shear forces for the steel and SE-SMA RC walls. Considering the seismic hazard  $S_{a(\text{design})}$ , the bending moments for the walls of BL1, BL1SW, and BL1SWF exceed the design moments by a factor of about 1.2, whereas the bending moments for the walls of BL2, BL2SW, and BL2SWF remain below the design moments. At the base, the wall bending moments for SMA RC dual systems are about 10% less than the moments for steel RC dual systems. The mean wall shear forces are below the design shear forces assuming  $R_d R_0 = 1.0$ . The shear forces are decreased in BL2SW and BL2SWF dual systems by about 6%.

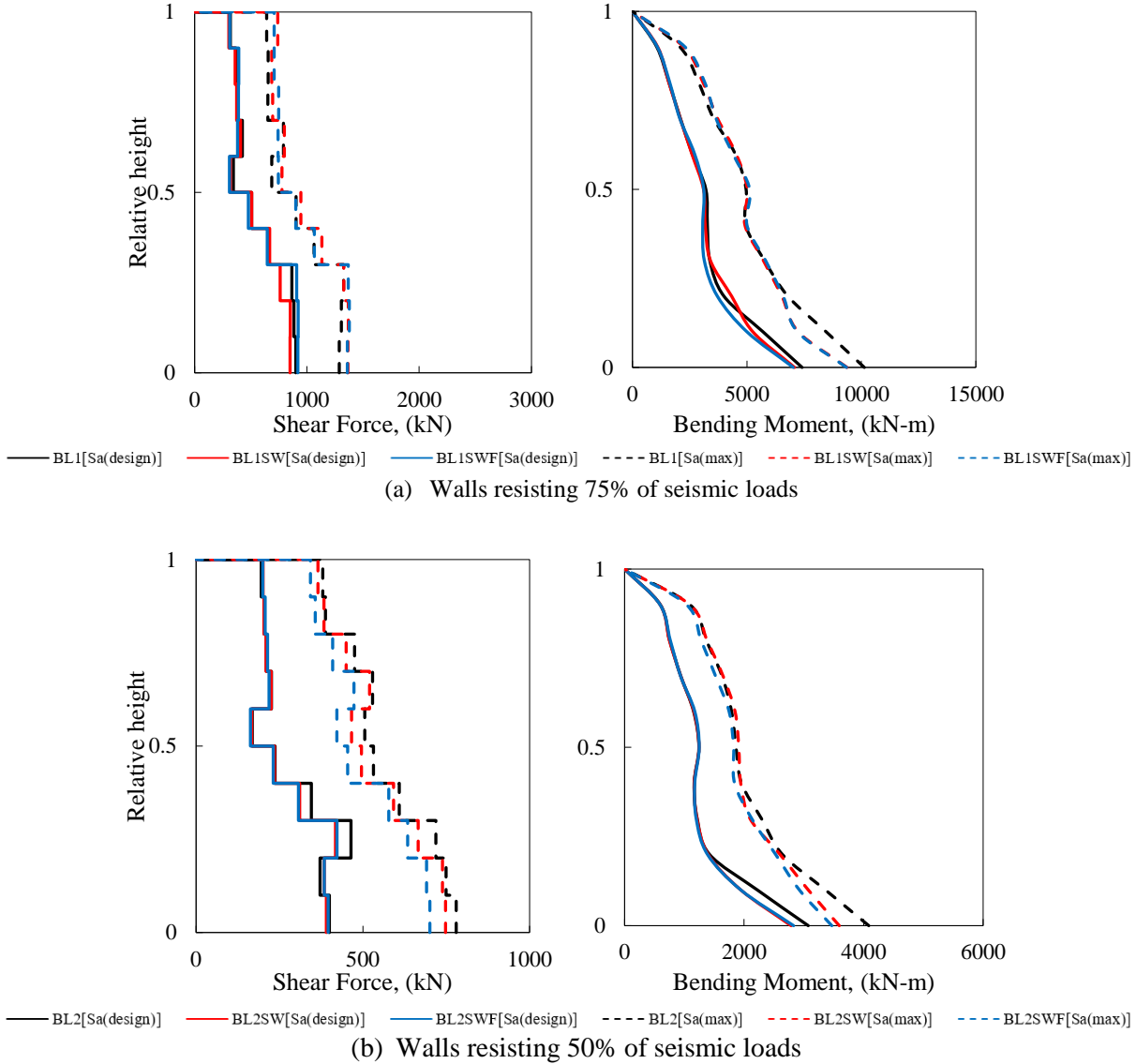


Figure 7. Mean shear force and bending moment envelopes in the RC walls

**4.2 Frame Local Response**

The mean tensile strains of the longitudinal bars of the external and internal beams are plotted in Figure 8. For seismic hazard  $S_{a(\text{design})}$ , RC beams are in the elastic strain stage. However, for seismic hazard  $S_{a(\text{max})}$ , inelastic strains are developed in the RC beams, reaching values of about 0.003. A small increase of about 6% in the strains is noted for BL1SWF and BL2SWF as compared to BL1SW and BL2SWF.

Figure 8 also shows the mean tensile strains of the longitudinal bars of the exterior columns. Inelastic strains are developed at the base of the columns for seismic hazard  $S_{a(\text{max})}$ . The influence of utilizing

SE-SMA bars is pronounced in BL1SWF, where the strains in the external columns have remained elastic.

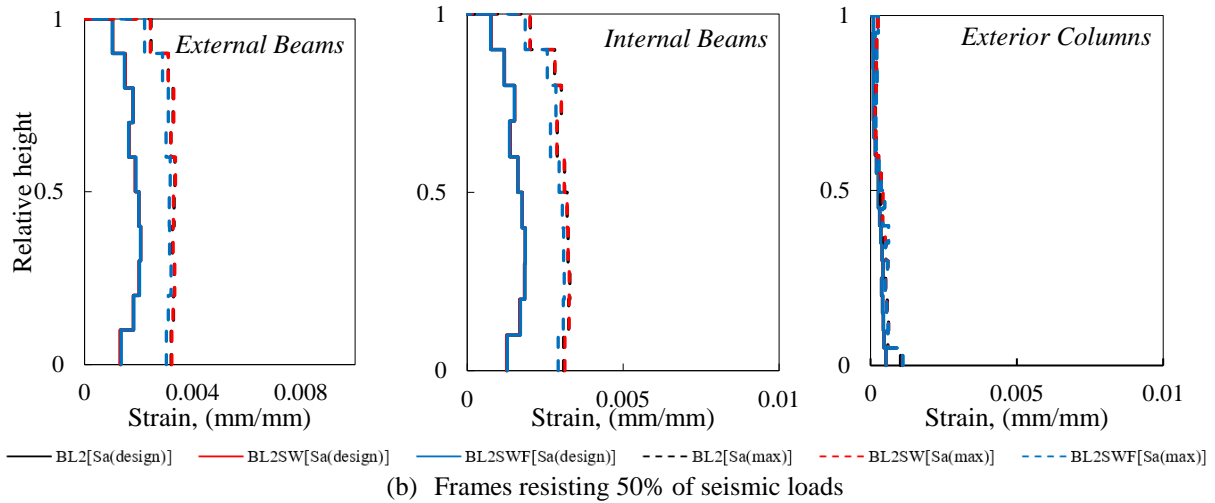
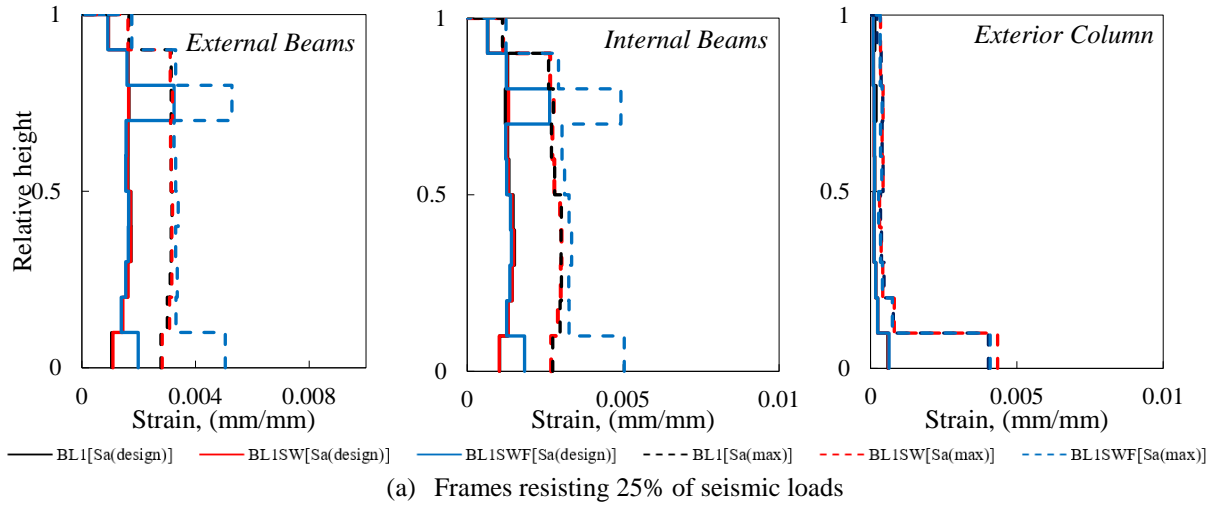


Figure 8. Mean strains envelopes in RC frame

The exterior column axial load ratios are presented in Figure 9. Increasing the seismic hazard from  $S_{a(\text{design})}$  to  $S_{a(\text{max})}$  increases the axial load ratio by 44%. Considering a seismic hazard of  $S_{a(\text{max})}$ , the axial load ratio for BL1SWF is 9% less than the BL1 and BL1SW.

Figure 9 also shows the shear forces in the external columns. Assuming  $R_d R_0 = 1.0$ , the design shear force at the base of the external column is 123 kN, which is 25% lower than the computed shear forces considering seismic hazards of  $S_{a(\text{design})}$ . The SE-SMA reduced the shear forces at the column base of BL1SWF and BL2SWF by about 17%. The difference in the shear forces at the upper stories is negligible. Considering seismic hazard  $S_{a(\text{max})}$ , the external column base shear forces of BL1 and BL2 is 169 and 184 kN, respectively, whereas the shear force is 126 kN for BL1SWF.

Lastly, Figure 9 shows the bending moments in the external columns. For BL1, they reach 493 kN.m and 1069 kN.m at  $S_{a(\text{design})}$  and  $S_{a(\text{max})}$ , respectively, while, for BL2, they reach 783 kN.m and 1600 kN.m, respectively. The base bending moment for BL2 exceeds the design moment by 29% at  $S_{a(\text{max})}$  hazard level. Utilizing SE-SMA bars in BL1SWF and BL2SWF reduce the base bending moment by about 18% considering seismic hazard  $S_{a(\text{max})}$ .

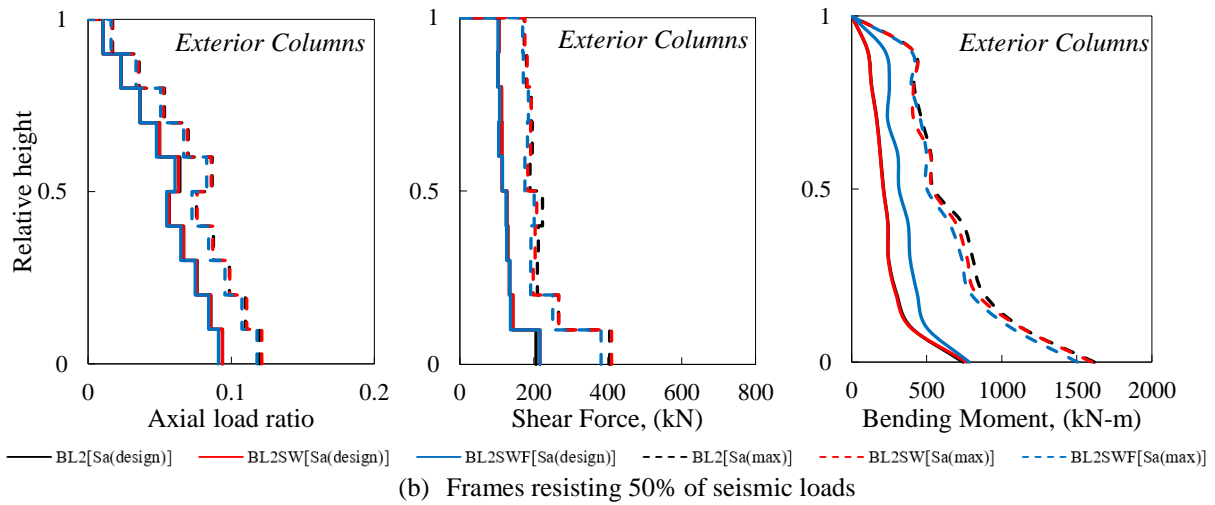
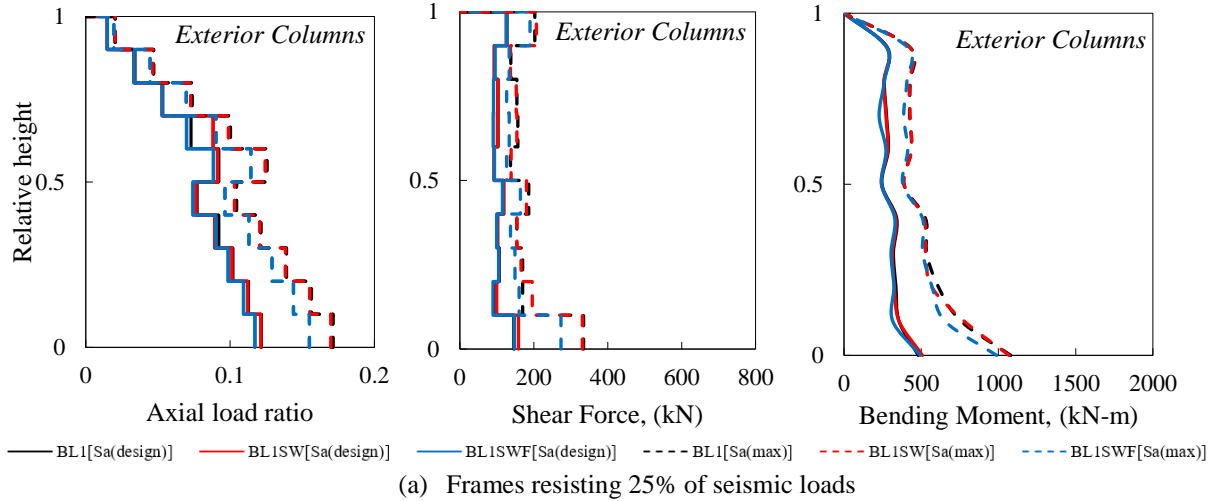


Figure 9. Mean axial, shear, and bending moment envelopes for RC exterior columns

### 4.3 System Global Response

Figure 10 presents the inter-story drift distribution along the height. Regardless of the type of reinforcement, the considered dual systems exhibit similar distribution of inter-story drifts considering low-intensity ground motions. The peak inter-story drift is reduced by 10% on average when the SE-SMA bars are used at the beam ends.

Figure 11 displays the mean residual displacements. SMA RC dual systems have the lowest residual displacements as compared to steel RC dual systems. At low seismic intensity, utilizing SE-SMA bars at the beam ends reduces the roof residual displacement by 37% and 15% for BL1SWF and BL2SWF, respectively. By increasing the intensity levels from the design level to the ultimate level, the residual displacements are reduced by 67% and 28% for BL1SWF and BL2SWF, respectively, as compared to BL1 and BL2.



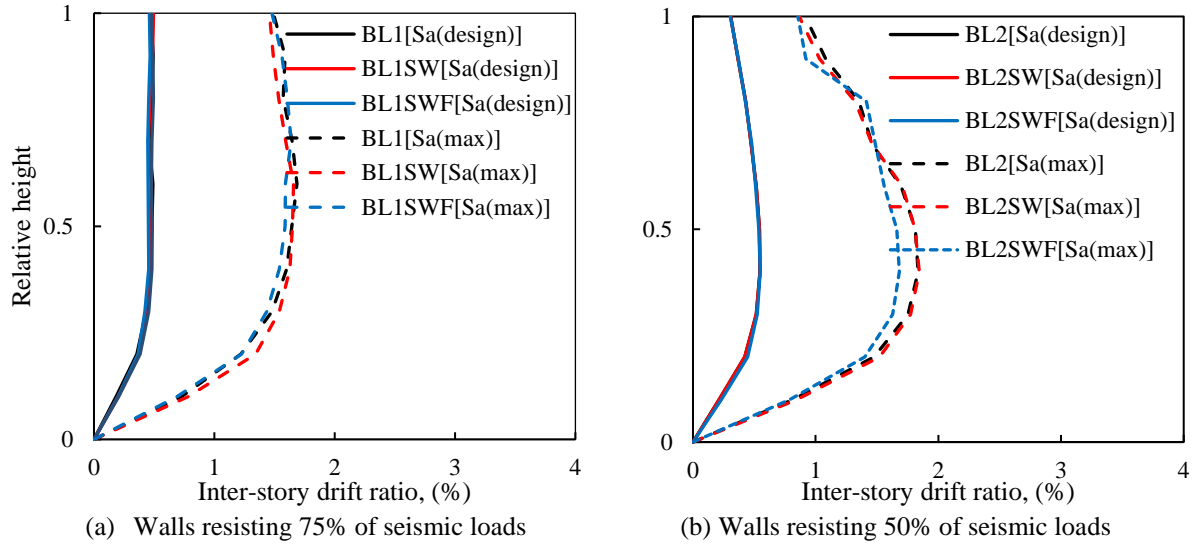


Figure 10. Mean inter-story drift ratios

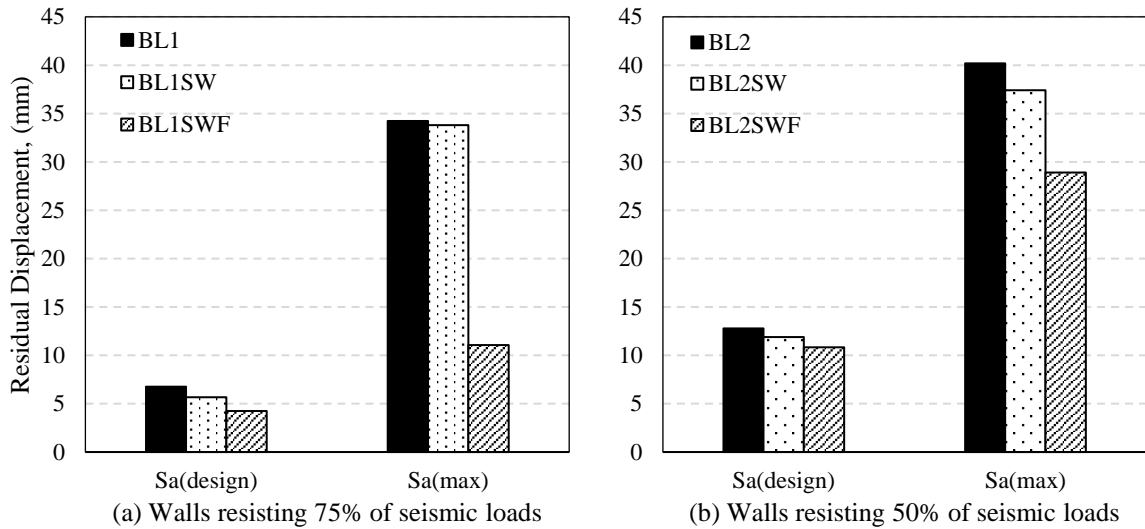


Figure 11. Mean residual displacements

## 5. CONCLUSIONS

This paper investigates the seismic performance of 10-story SE-SMA RC dual systems. Two groups of buildings are designed based on the stiffness ratio of the RC walls to the ductility moment frames. The considered buildings are assumed to be located in the high seismic zone of Vancouver, BC. The investigation has led to the following conclusions:

1. A single plastic hinge is developed at the base of RC walls at  $S_{a(max)}$  hazard level. The length of the formed plastic hinge is about 10% of total wall height.
2. At seismic hazard  $S_{a(design)}$ , no notable difference is observed in the strain distributions of the RC beams and RC columns at the locations of SE-SMA.

3. At seismic hazards of  $S_{a(max)}$ , the use of SE-SMA bars has reduced the shear forces of the external columns by about, 18% for BL1SW and BL1SWF, whereas a small reduction in the shear forces is noted for BL2SW and BL2SWF.
4. There is no difference in the wall bending moments between SE-SMA and steel dual-systems at seismic hazard  $S_{a(design)}$ . Considering seismic hazard  $S_{a(max)}$ , utilizing SE-SMA bars in the dual systems reduces the wall bending moments at the base by about 10% as compared to BL1 and BL2.
5. A negligible difference is noted in the mean inter-story drifts when SE-SMA bars are introduced.
6. Time history analysis has confirmed that the residual drifts are reduced significantly, when the SE-SMA bars are utilized.

## 6. REFERENCES

- The National Building Code of Canada (1985). Ottawa: Canadian Commission on Building and Fire Code, National Research Council.
- Emori, K., & Schnibrich, W (1978). Analysis of reinforced concrete frame-wall structures for strong motion earthquake. *Structural research series* no 434.
- Goodsir, W., Paulay, T., & Carr, A (1982). The inelastic seismic response of reinforced concrete frame-shear-wall structures. Christchurch, New Zealand: University of Canterbury.
- Aktan, A., & Bertero, V. (1984). Seismic response of R/C frame-wall structures. *Journal of Structure Engineering*, 110(8): 1803-1821.
- Tuna, Z. (2012). Seismic performance, modeling, and failure assessment of reinforced concrete shear wall buildings, *Ph.D thesis*, University of California, Los Angeles, USA.
- Youssef, M., Alam, M., & Nehdi, M (2008). Experimental investigation on the seismic behaviour of beam-column joints reinforced with superelastic shape memory alloys. *Journal of Earthquake Engineering*, 12(7), 1205-1222.
- Saiidi, S., O'Brien, M., & Sadrossadat-Zade, M (2008). Cyclic Response of Concrete Bridge Column Using Superelastic Nitinol and Bendable Concrete. *ACI Structural Journal*: 106(1), 69-77.
- Alam, M., Youssef, M. A., & Nehdi, M. (2008). Analytical prediction of the seismic behaviour of superelastic shape memory alloy reinforced concrete elements. *Engineering Structures*: 30(12), 3399-3411.
- Tazarv, M., & Saiidi, M. (2013). Analytical studies of the seismic performance of a full-scale SMA-reinforced bridge column. *International Journal of Bridge Engineering*: 1(1), 37-50.
- Abdulridha, A. (2012). Performance of superelastic shape memory alloy reinforced concrete elements subjected to monotonic and cyclic loading. *Ph.D thesis*: University of Ottawa, Ottawa, Canada
- Abraik, E., & Youssef, M. (2015). Cyclic performance of shape memory alloy reinforced concrete walls. Response of structures under extreme loading (pp. 326-333). Lansing, MI: *The fifth international workshop on performance, protection, and strength of structures under extreme loading*.
- Abraik, E., & Youssef, M. (2016). Performance assessment of three-story shape memory alloy reinforced concrete walls. *CSCE 5th International Structural Specialty Conference*, 852. London, ON, Canada.

- Open system for earthquake engineering simulation (OpenSees). PEER, University of California, Berkeley, CA, 2004.
- Kolozvari, K (2013). Analytical Modeling of cyclic shear-flexural interaction in reinforced concrete structural walls. *Ph.D thesis*: University of California, Los Angeles, USA.
- PEER-TBI (2017). Guidelines for performance-based seismic design of tall buildings, Report No. 2010/05. Pacific Earthquake Engineering Research Center, University of California, Berkeley, CA.
- Panagiotou, M (2008). Seismic design, testing, and analysis of reinforced concrete wall buildings. *Ph.D thesis*, University of California, San Diego, USA.
- Hurlebaus, S., & Gaul, L (2006). Smart structure dynamics. *Mechanical system and signal*: 20(2), 255-281.
- Ghorbanirenani, I., Tremblay, R., Léger, P., & Leclerc, M (2012). Shake table testing of slender RC shear walls subjected to Eastern North America seismic ground motions. *Journal of Structural Engineering*: 138(12), 1515-1529.
- The National Building Code of Canada (2005). Ottawa: Canadian Commission on Building and Fire Code, National Research Council.
- The National Building Code of Canada (2015). Ottawa: Canadian Commission on Building and Fire Code, National Research Council.